frontiers | Frontiers in Environmental Science

ORIGINAL RESEARCH
published: 13 June 2022
doi: 10.3389/fenvs.2022.903013

Developing Nitrogen Isotopic Source Profiles of Atmospheric Ammonia for Source Apportionment of Ammonia in Urban Beijing

Chenjing Wang[1,2,3], Xiujuan Li[1], Tianle Zhang[2], Aohan Tang[1], Min Cui[2,4], Xuejun Liu[1], Xin Ma[1], Yangyang Zhang[1], Xiaomeng Liu[2] and Mei Zheng[2]**

[1]Beijing Key Laboratory of Farmland Soil Pollution Prevention and Remediation, College of Resources and Environmental Science, China Agricultural University, Beijing, China, [2]State Key Joint Laboratory of Environmental Simulation and Pollution Control, College of Environmental Sciences and Engineering, Peking University, Beijing, China, [3]Beijing Key Laboratory of Airborne Particulate Matter Monitoring Technology, Beijing Municipal Ecological and Environmental Monitoring Center, Beijing, China, [4]College of Environmental Science and Engineering, Yangzhou University, Yangzhou, China

OPEN ACCESS

Edited by:
Junwen Liu,
Jinan University, China

Reviewed by:
Woo-Jung Choi,
Chonnam National University, South Korea
Yu-Chi Lin,
Nanjing University of Information Science and Technology, China

***Correspondence:**
Aohan Tang
aohantang@cau.edu.cn
Mei Zheng
mzheng@pku.edu.cn

Specialty section:
This article was submitted to Atmosphere and Climate, a section of the journal Frontiers in Environmental Science

Received: 23 March 2022
Accepted: 29 April 2022
Published: 13 June 2022

Citation:
Wang C, Li X, Zhang T, Tang A, Cui M, Liu X, Ma X, Zhang Y, Liu X and Zheng M (2022) Developing Nitrogen Isotopic Source Profiles of Atmospheric Ammonia for Source Apportionment of Ammonia in Urban Beijing. Front. Environ. Sci. 10:903013. doi: 10.3389/fenvs.2022.903013

Atmospheric ammonia (NH_3) is the key precursor in secondary particle formation, which is identified as the most abundant components of haze in Beijing in most cases. It is critical to understand the characteristics of NH_3 from various emission sources and quantify each source contribution to NH_3 in ambient atmosphere. Stable nitrogen (N) isotope composition ($\delta^{15}N$) is an effective tool to study NH_3 source. However, this tool cannot be effectively applied in Beijing due to the lack of comprehensive N nitrogen isotope source profiles. Reliable source profiles are the basis of source apportionment of NH_3 using the isotope mixing model. In this study, multiple NH_3 source samples were collected at sites, representing six major NH_3 source types in Beijing from 2017 to 2018 in four seasons. The $\delta^{15}N$ values of 212 NH_3 source samples were determined to build a local source profiles database of $\delta^{15}N$. NH_3 from traffic source presents significantly higher $\delta^{15}N$ values (−14.0 ± 5.4‰), distinguished from other sources. The $\delta^{15}N$ values of other sources besides traffic were more depleted and did not clear differences (solid waste, sewage, human feces, fertilizer, and livestock for −33.6 ± 4.5‰, −34.1 ± 4.8‰, −32.2 ± 3.8‰, −35.0 ± 3.9‰, and −34.9 ± 4.4‰, respectively). These sources were classified into non-traffic source in this study. From March 2018 to March 2019, ambient NH_3 samples were collected at an urban site in Beijing. With the newly developed source profiles in this study, the contribution of traffic and non-traffic sources to ambient NH_3 in an urban site in Beijing was calculated using ^{15}N isotope mass balance equations. Traffic and non-traffic sources contributed 8% and 92% to ambient NH_3 in urban Beijing, respectively. The highest seasonal average contribution of traffic to ambient NH_3 was found in winter (22%). Our results reveal the importance of traffic source and provide evidence for the need to control NH_3 emission from traffic in urban Beijing in winter.

Keywords: ammonia, nitrogen isotope, source profile, source apportionment, Beijing

1 INTRODUCTION

Due to the intensive human activities of past decades, severe fine particle ($PM_{2.5}$) pollution occurred frequently in China, especially in the North China Plain (NCP). $PM_{2.5}$ pollution has known impacts on climate, visibility, radiation budget, and human health (Sun et al., 2006). It has been reported by previous studies that secondary inorganic aerosol (sulfate, nitrate, and ammonium) is a major contributor to $PM_{2.5}$ during haze periods (Huang et al., 2014; Tian et al., 2014). As the only alkaline gaseous precursor of $PM_{2.5}$ in the atmosphere, NH_3 plays an important role in $PM_{2.5}$ formation. NH_3 can neutralize acid species, such as nitric acid and sulfuric acid, forming secondary aerosols (Ansari and Pandis, 1998; Kirkby et al., 2011; Behera et al., 2013). Studies showed that NH_3 emissions have been increased since 1980 (Liu et al., 2013; Warner et al., 2017; Zhang et al., 2017), and the NCP was a hotspot area with high NH_3 concentration in China (Xu et al., 2015; Pan et al., 2018b). It has been proposed that reducing NH_3 could be a more effective method for haze mitigation in the NCP (Pan et al., 2016). Quantifying NH_3 emission sources and estimating the contribution from each key source in Beijing is not only urgent but also challenging.

NH_3 in the atmosphere is mainly emitted from anthropogenic sources, such as agricultural activities (fertilizer application and livestock manure), traffic, coal combustion, urban waste (like solid waste, sewage, and human feces), and biomass burning (Sutton et al., 2000; Behera et al., 2013; Chang, 2014; Li et al., 2017). It is widely accepted that livestock manure and fertilizer application are the most important sources of NH_3, accounting for approximately 60–80% to global NH_3 emission budget (Bouwman et al., 1997; Holland et al., 1999; Paulot et al., 2014; Liu et al., 2022). NH_3 emission source inventory over China suggested that agricultural source was the dominated source (Huang et al., 2012; Paulot et al., 2014; Kang et al., 2016; Zhang et al., 2017). Nevertheless, some studies argued that non-agricultural source could be underestimated in the urban area, which received increasing attention in recent years (Chang et al., 2016; Pan et al., 2016; Chang et al., 2019). There is still controversy over the source contribution of NH_3 in cities.

Stable nitrogen isotope composition ($\delta^{15}N$) here refers to the ratio of $^{15}N/^{14}N$ in NH_3 relative to atmospheric N_2 calculated in parts per thousand, which has been applied as an effective tool to identify NH_3 sources. Since NH_3 emitted from different sources have different $\delta^{15}N$ values (Chang et al., 2016), sources of NH_3 at a site can be identified through the analysis of $\delta^{15}N$ of ambient NH_3 and quantified further with the help of an isotope mixing model. According to published data, $\delta^{15}N$-NH_3 source signatures of coal combustions (−25.5 to −11.3‰) and urban traffic (−14.9 to 6.3‰) were found to be significantly different from agricultural sources, such as fertilizer application (−52.0 to −26.4‰) and livestock (−38.3 to −10.5‰) (Felix et al., 2013; Chang et al., 2016; Savard et al., 2017; Ti et al., 2018; Stratton et al., 2019; Bhattarai et al., 2020; Walters et al., 2020; Song et al., 2021). $\delta^{15}N$-NH_3 source signatures of urban waste, like solid waste (−36.6 to 7.8‰), sewage (−41.3 to −35.7‰), and human feces (−38.4 to −38.6‰) were reported to be similar to $\delta^{15}N$-NH_3 of agricultural sources (Chang et al., 2016; Liu et al., 2016).

Previous studies in some regions have reported the $\delta^{15}N$ value of ambient NH_3 (Moore, 1977; Hayasaka et al., 2011; Buzek et al., 2017; Felix et al., 2017) and quantified the source of NH_3 or NH_4^+ in particle using the isotope mixing model (Chang et al., 2016, 2019; Pan et al., 2016, 2018a; Ti et al., 2018). Since 2016, some reports on the source apportionment of NH_3 using $\delta^{15}N$-NH_3 have been published (Chang et al., 2016; Pan et al., 2016, 2018a; Bhattarai et al., 2020; Zhang et al., 2020; Gu et al., 2022), which helped researchers in reassessing the contribution of non-agricultural sources to NH_3 in urban Beijing. The accuracy of such estimation heavily relies on well-established source profiles of $\delta^{15}N$-NH_3. Localized source profiles, containing the $\delta^{15}N$-NH_3 signatures of traffic, urban waste, fertilizer application, and livestock have been reported in Shanghai, China (Chang et al., 2016), and Colorado, United States (Stratton, et al., 2019). Several studies published their results of $\delta^{15}N$-NH_3 values of traffic in Shenyang, China (6.3‰, Song et al., 2021), Albert, Canada (−14.9‰, n = 4, Savard et al., 2017), Providence, United States (6.6 ± 2.1‰, Walters et al., 2020), and Pittsburgh, United States (−4.6‰ and −2.2‰, Felix et al., 2013). For agricultural sources, $\delta^{15}N$-NH_3 values of fertilizer application in cropland was also measured in the Taihu area, China (−30.8 to −3.3‰), Maryland, United States (−48.0 to −36.3‰), and Alberta, Canada (−31.3‰). NH_3 emitted from livestock manure in the pig farm (−30.1 to −10.5‰), dairy farm (−28.5 to −11.3‰), cattle farm (−38.3%), and the turkey farm (−36.0 to −56.1‰) were reported in the Taihu area, China (Ti et al., 2018), Alberta, Canada (Savard et al., 2017), and Maryland, Kansas, and western Pennsylvania in the United States (Felix et al., 2013). There were not too many published data on $\delta^{15}N$-NH_3 values of urban waste. The $\delta^{15}N$-NH_3 values of agricultural sources like fertilizer application (−40.4 ± 5.3‰, Bhattarai et al., 2020) and livestock (−29.78 to −14.05‰, Liu et al., 2016), urban waste sources like landfill (−19.14 to 7.82‰, Liu et al., 2016) were measured in Beijing as well. The $\delta^{15}N$-NH_3 signatures, especially for urban waste were still relatively limited in Beijing.

The main goal of this research is to establish local $\delta^{15}N$-NH_3 source profiles in urban Beijing to carry out source apportionment of NH_3 in ambient air. The $\delta^{15}N$ values of six NH_3 emission sources (traffic, solid waste disposal, sewage treatment, human feces disposal, fertilizer, and livestock) are reported in urban Beijing based on 212 NH_3 source samples. With the help of newly established source profiles, sources of ambient NH_3 were also identified and quantified at an urban site in Beijing.

2 MATERIALS AND METHODS

2.1 Sampling

2.1.1 Sampling Sites

Except for the well-known NH_3 sources like fertilizer and livestock (Kang et al., 2016), non-agricultural NH_3 source samples (traffic, solid waste disposal, sewage treatment, and human feces disposal) were also sampled in urban Beijing in this study. For traffic source, some studies have shown the importance of traffic for NH_3 in the urban area (Sun et al.,

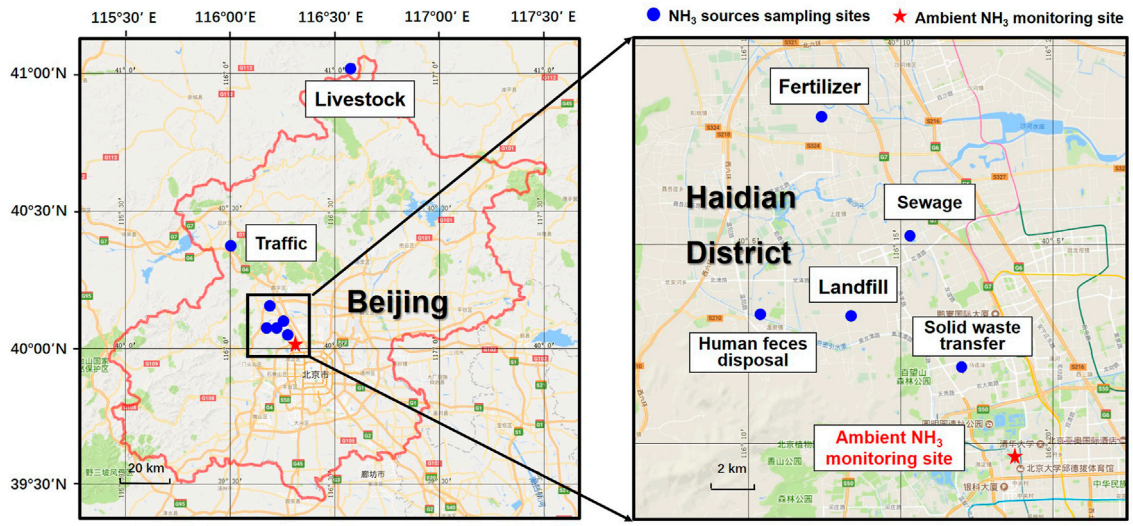

FIGURE 1 | The sampling locations of the NH_3 emission sources samples and ambient samples. The blue point indicates sites for collecting NH_3 source samples and the red pentagram shows the ambient air monitoring site.

2017). The emission inventory also suggests that urban waste (solid waste disposal, sewage treatment, and human feces disposal) could be important in cities with high-population density (Chang, 2014). Therefore, these sources were also included in this study.

NH_3 source samples were collected in four seasons from March 2017 to October 2018 at six sampling sites, including; 1) a crop site, located in the Shangzhuang experiment station, growing wheat in winter and corn in summer, and sampling was conducted at an acer of field where synthetic fertilizer was applied (120 kg N ha^{-1}) (Sha et al., 2020); 2) a livestock site, located in the Fengning experiment station, maintained about 4,000 pigs in average during the sampling period, and NH_3 samples were collected in three types of pig house (sow house, nursery house, and fattening house); 3) a traffic site, located in a 1,085 m-long Badaling tunnel, which is an ideal place to collect NH_3 emitted from vehicle exhaust, and emissions were from both gasoline cars and diesel vehicles including various personal and commercial vehicles; 4) two solid waste disposal sites, one site located in the Liulitun landfill, with the daily landfill volume as 887 tons in 2017 (NH_3 samples were collected at both the leachate treatment room and the landfill area), and the other was located in a solid waste transfer station in China Agricultural University; 5) a sewage treatment site, located in the Yongfeng sewage treatment plant, had a daily throughput of 1.98×10^4 m^3, and NH_3 samples were collected in a secondary sedimentation tank, oxidation ditch, and fine grid room; and 6) a human feces disposal site, located in the Sanxingzhuang human feces disposal station, had a daily fecal fluid throughput of 400 t, and NH_3 samples were collected in the fecal wastewater treatment tank and the fecal residue storage room. The locations of sampling sites are shown in **Figure 1**. More detailed information of sampling sites can be found in **Supplementary Table S1**.

In addition to source samples, ambient NH_3 samples were collected from March 2018 to March 2019. The monitoring site was set in the campus of Peking University (39°59′N, 116°18′E, PKU). It is a typical urban site in northwest of Beijing city, surrounded by residential buildings, teaching buildings, and parks, with dense population and traffic. There are no significant industrial emission sources near the site.

2.1.2 Sample Collection

In this study, the ALPHA passive sampler was used to collect NH_3 source samples and ambient NH_3 samples (Adapted Low-cost Passive High Absorption, CEH, Center for Ecology and Hydrology), which has been applied in many studies to measure NH_3 concentration and $\delta^{15}N$ values (Tang et al., 2001; Skinner et al., 2004; Felix et al., 2013; Chang et al., 2016; Felix et al., 2017; Xu et al., 2017). The ALPHA sampler is a circular polyethylene vial (26 mm height, 27 mm diameter) with one open end, containing a 24 mm citric acid impregnated filter and a PTFE (Teflon) membrane for gaseous NH_3 diffusion (**Supplementary Figure S1**). The typical sampling duration for most NH_3 sources and ambient NH_3 was usually about 1 week. For livestock, NH_3 source sampling duration was 1 day. The sampling duration of the third sample of ambient NH_3 in June and the first ambient NH_3 samples in February 2019 were more than 2 weeks. The detection limit of ALPHA is 0.02 μg/m^3.

At each site, the ALPHA sampling system (consisting of three ALPHA samplers) was placed at about 1.5 m above ground (ambient NH_3 samples were collected at 20 m above ground in the roof of a teaching building), and under a PVC shelter to prevent sampler from rain and sunlight (**Supplementary Figure S1**). A total of 212 NH_3 source samples and 45 ambient NH_3 samples were collected and analyzed in this study. To avoid contamination, the NH_3 absorbent was freshly prepared on the day of sampling. Collected NH_3 samples were stored at 4°C until analysis. Three field blanks were prepared for each batch of samples (about 50 samples). These field blanks were brought to each sampling site without installing on the sampler and then

transported back to the laboratory. Along with NH_3 source samples and ambient NH_3 samples, NH_3 concentrations of field blanks were analyzed to assess potential contamination during laboratory preparation and sample transport between the field and the laboratory. All the concentration data reported in the following text were subtracted with blank.

2.2 Chemical Analysis

Before sampling, the filter was impregnated in the absorbent, which was made by citric acid dissolved in methanol. After sampling, NH_3 collected in the filter was extracted with ultrapure water (18.2 MΩ cm, Milli-Q system), and then analyzed as NH_4^+ by using a continuous-flow analyzer (Seal AA3, Germany). The detection limit was 0.1 mgN/L. The analysis of NH_4^+ concentration was conducted at the Key Laboratory of Plant–Soil Interactions, Chinese Ministry of Education, China Agricultural University.

The $\delta^{15}N$ analysis was performed at the Stable Isotope Ecology Laboratory of Institute of Applied Ecology, Chinese Academy of Sciences, by following the method of Liu et al. (2014). First, NH_4^+ in leaching liquor was oxidized to NO_2^- by BrO^-, and then, NO_2^- was quantitatively converted into N_2O by reductant under strong acid condition. The performance of the reduction of NO_2^- to N_2O was evaluated by measuring the laboratory standard ($NaNO_2$, −11.7‰, determined by EA-IRMS). The produced N_2O was finally collected by a purge and cryogenic trap system (Gilson GX-271, IsoPrime Ltd., Cheadle Hulme, United Kingdom) and the $\delta^{15}N$ values were determined on an IRMS (PT–IRMS) (IsoPrime 100, IsoPrime Ltd., Cheadle Hulme, United Kingdom). In this study, the first 119 source samples (collected from March 2017 to January 2018) were analyzed using hydroxylamine (NH_2OH) as the reductant. In order to shorten the conversion time of NO_2^- to NO_2 (from 16 h to 4 h), sodium azide (NaN_3) was used as reductant when the last 93 source samples (collected from March to October in 2018) and ambient samples were analyzed in the laboratory (**Supplementary Table S1**). There was no significant influence of isotopic fraction on isotope analysis for changing reductant because NO_2^- was fully quantitatively converted into N_2O by checking the measured $\delta^{15}N$ value of laboratory $NaNO_2$ standards. Three international reference standards (IAEAN1, USGS25, and USGS26 with $\delta^{15}N$ values of +0.4, −30.4, and +53.7‰, respectively) were used for calibration. The details of analytical procedures are also given elsewhere (Liu et al., 2014).

2.3 Calculation

The concentration of NH_3 (C, μg/m^3) was calculated as follows:

$$C = (m_e - m_b)/V,$$

where m_e and m_b represent the amount of NH_3 (μg) collected on sample and blank sample, respectively; V is the effective sampled air volume (V, m^3) by the ALPHA sampler, which is determined by the sampling time and the sampling rate of the sampler. V is calculated by the following equation:

$$V = DAt/L,$$

where t represents the time of filter exposure to collect NH_3 gas (h); D is the diffusion parameter, $D = 2.09 \times 10^{-5}$ m^2/s at 10°C; A represents the sampling area (m^2) of the filter, $A = 3.4636 \times 10^{-4}$ m^2; L is the diffusion length (m) from the membrane to the filter, L = 0.006 m.

The N isotope composition ($\delta^{15}N$) is reported in parts per thousand relative to atmospheric N_2 as follows:

$$\delta^{15}N\,(‰) = \frac{(^{15}N/^{14}N)_{sample} - (^{15}N/^{14}N)_{standard}}{(^{15}N/^{14}N)_{standard}} \times 1000,$$

where ^{15}N and ^{14}N are the atomic mass of 15 and 14, respectively; $^{15}N/^{14}N$ represents the ratio of nitrogen isotope.

The calibration equation of $\delta^{15}N$ is as follows:

$$\delta^{15}N_{corrected} = \frac{\delta^{15}N_{measured} - intercept}{slope},$$

where $\delta^{15}N_{corrected}$ is the corrected values of NH_3 sample; $\delta^{15}N_{measured}$ is the measured values of NH_3 sample; the intercept and slope are from the linear regression of the measured $\delta^{15}N$ values of standards and the assigned $\delta^{15}N$ values of standards (Liu et al., 2014).

Only traffic source was significantly distinguished from other sources in the $\delta^{15}N$-NH_3 value, while sewage, solid waste, human feces, fertilizer, and livestock did not significantly differ from each other. Therefore, those sources that could not be significantly distinguished in $\delta^{15}N$-NH_3 values were lumped together as one category (non-traffic source). The contribution of traffic source and non-traffic source to ambient NH_3 can be calculated as follows:

$$\delta^{15}N_{ambient} = f_{traffic} \times \delta^{15}N_{traffic} + f_{non-traffic} \times \delta^{15}N_{non-traffic}$$
$$f_{traffic} + f_{non-traffic} = 1,$$

where $\delta^{15}N_{ambient}$ is the observed values of ambient NH_3; $\delta^{15}N_{traffic}$, and $\delta^{15}N_{non\text{-}traffic}$ are the measured values of NH_3 from traffic and non-traffic source; $f_{traffic}$ and $f_{non\text{-}traffic}$ are the contribution fraction of traffic and non-traffic source to ambient NH_3.

2.4 Statistical Analysis

To evaluate the differences in mean $\delta^{15}N$ signatures and concentrations among NH_3 sources, one-way ANOVA followed by the Student–Newman–Keuls test (S–N–K) was carried out for *post hoc* multiple comparison at a 5% level of significance. One-way ANOVA was also used to determine any seasonal difference in mean $\delta^{15}N$-NH_3 signatures and concentrations among NH_3 sources and ambient NH_3. For traffic and fertilizer application, Kruskal–Wallis test was conducted to evaluate whether or not there is statistically significant difference between the medium values of $\delta^{15}N$ values and NH_3 concentrations. The statistical analyses were performed using SPSS Version 25.0.

3 RESULTS AND DISCUSSION

3.1 Source Profile of Ammonia Emission Source

3.1.1 Ammonia Concentration in Emission Sources

It can be seen that there is a wide range in NH_3 concentration among sources from 3.4 to over 8,000 μg/m^3 (**Figure 2**). The highest average NH_3 concentration was found in the livestock farm (3,317.0 ± 2,316.0 μg/m^3, n = 34), about 20 times and 70 times higher than

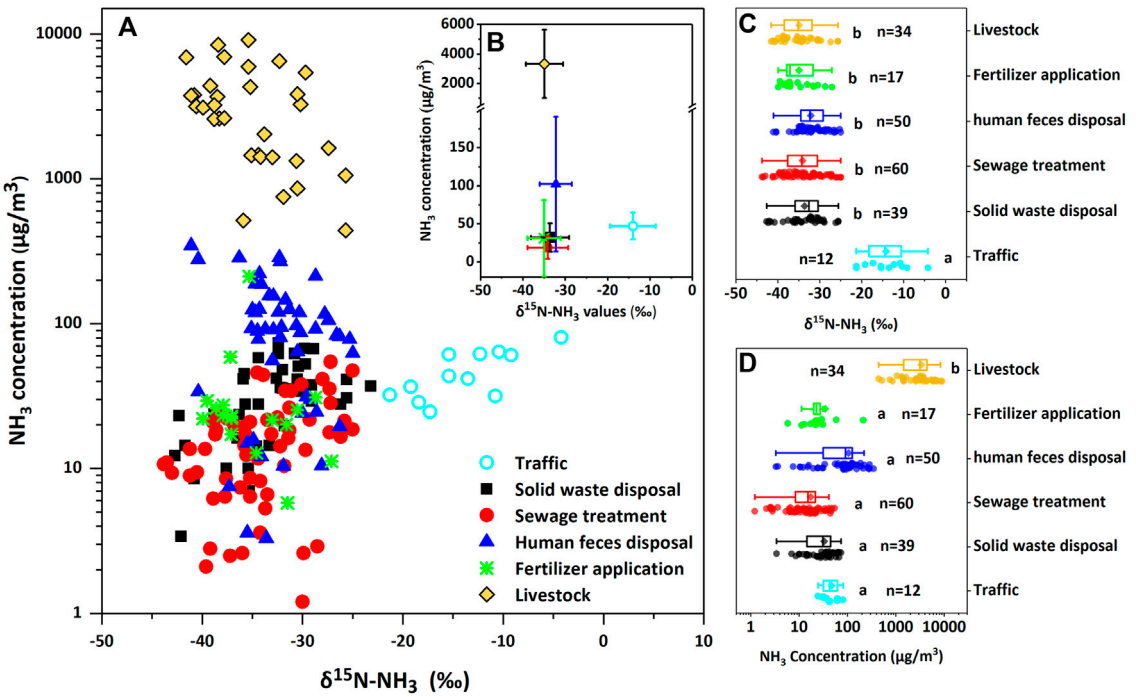

FIGURE 2 | The relationship between NH_3 concentration and $\delta^{15}N$-NH_3 values of each source samples in Beijing. **(A)** shows the $\delta^{15}N$-NH_3 values plotted against NH_3 concentration of each source samples. **(B)** shows the mean $\delta^{15}N$-NH_3 values and mean concentration of each sources, error bars indicate standard deviation of each mean. **(C,D)** are box-plots of δ15N- values and concentration of each sources respectively, the square and line within the box represent the mean and median values of $\delta^{15}N$-NH_3 values and concentration, the left and right edges of the box represent the 25th and 75th percentiles of $\delta^{15}N$-NH_3 values and concentration, the left and right bars represent the min and max values, different letters adjacent the bars indicate difference among NH_3 sources ($p < 0.05$).

human feces (102.3 ± 88.5 μg/m^3, n = 50) and fertilizer (31.1 ± 50.3 μg/m^3, n = 17), respectively. The mean concentration of NH_3 emitted from livestock was significantly different from other five sources ($p < 0.05$). Larger amount of urea, a kind of volatile nitrogen compound, in livestock and human feces could be responsible for high NH_3 concentration (Sha et al., 2020). In addition, NH_3 samples for livestock and fecal residue were collected indoor in this study, so the enclosed space resulted in high NH_3 accumulation. Large emission of NH_3 from urea fertilizer was also detected in this study. NH_3 concentration could reach up to 212.3 μg/m^3 in the first 3 days after fertilizer application in corn field in summer. For solid waste disposal and sewage treatment (32.0 μg/m^3 and 18.8 μg/m^3, respectively), the mean concentration was lower than that in other sources. The average NH_3 concentration in traffic source was the third highest (47.2 μg/m^3, n = 12), as the result of the large traffic volume and the semi-enclosed space in the tunnel. It also provides evidence that traffic could be an important source of NH_3.

NH_3 concentration measured at pig barns in this study was similar to the results of other observations in China (2,369 μg/m^3, n = 27, Beijing, Liu et al., 2016; 1,329.6 μg/m^3, n = 4, Shanghai, Chang et al., 2016). It was about 20 times higher than that observed for cow and turkey (51.6–165.6 μg/m^3, n = 7, Felix et al., 2013), since the ventilation of the pig farm in our sampling site is poor. For human feces disposal, NH_3 concentration was about 40 times lower than that determined in the septic tank (over 4,000 μg/m^3, n = 8, Chang et al., 2016). In the study of Chang et al. (2016), large amounts of NH_3 accumulated in the enclosed septic tank results in higher NH_3 concentration, in contrast to less nitrogen compound after treatment in fecal residue and fecal wastewater in this study. In the perspective of fertilizer application, the average concentration of NH_3 collected in cropland for fertilizer application was close to that determined in the wheat field (27.5 μg/m^3) but much lower than the rice field (99.3 μg/m^3) (Ti et al., 2018). It is due to significantly higher NH_3 volatilization for rice paddy than wheat land (Huang et al., 2016).

NH_3 concentrations exhibited distinct seasonal variations for six sources (**Supplementary Figure S2**). In most sources, the concentration was higher in spring and summer than other seasons, especially winter. For solid waste disposal and sewage treatment, NH_3 concentration in spring and summer was statistically significantly different from fall and winter ($p < 0.05$). Significant difference was also found in fertilizer application. The mean concentration was significantly higher in summer than in spring ($p < 0.05$). The temperature could be a major influencing factor. Higher temperature in summer could enhance the NH_3 volatilization from emission source. However, livestock source exhibits different seasonal variation. The highest NH_3 concentration was found in winter (7,341.5 ± 1,689.7 μg/m^3, n = 4) about seven times higher than the lowest concentration in summer ($p < 0.05$). In winter, all the windows were closed to maintain indoor temperature high and save energy. Since ambient temperature was high in summer,

TABLE 1 | $\delta^{15}N$ values and NH_3 concentration of six NH_3 emission sources in Beijing.

Source type	Season	N	$\delta^{15}N$ (‰)		Concentration (μg/m^3)	
			By season	Annual avg.	By season	Annual avg.
Traffic	Spring	2	−14.5 ± 1.3	−14.0 ± 4.9	42.5 ± 8.2	47.2 ± 17.8
	Summer	5	−10.3 ± 4.1		65.6 ± 8.5	
	Fall	2	−20.3 ± 1.5		34.5 ± 3.2	
	Winter	3	−15.5 ± 4.1		28.3 ± 3.5	
Solid waste disposal	Spring	14	−31.0 ± 3.1	−33.6 ± 4.5	40.5 ± 14.1	33.1 ± 18.9
	Summer	8	−31.5 ± 3.2		48.7 ± 21.4	
	Fall	12	−36.5 ± 4.3		24.3 ± 10.3	
	Winter	5	−37.4 ± 3.8		8.7 ± 4.0	
Sewage treatment	Spring	20	−32.1 ± 4.7	−34.1 ± 4.8	26.7 ± 10.7	17.3 ± 10.5
	Summer	11	−31.3 ± 3.5		24.6 ± 12.7	
	Fall	18	−37.8 ± 3.9		11.0 ± 4.3	
	Winter	11	−34.6 ± 3.9		3.5 ± 1.8	
Human feces disposal	Spring	17	−33.2 ± 4.9	−32.0 ± 4.6	149.1 ± 81.9	101.1 ± 83.9
	Summer	11	−28.9 ± 5.8		71.9 ± 68.9	
	Fall	15	−31.0 ± 4.7		83.6 ± 83.2	
	Winter	7	−33.5 ± 4.1		71.9 ± 75.4	
Fertilizer application	Spring	6	−32.2 ± 4.9	−35.0 ± 3.9	16.7 ± 8.9	31.1 ± 50.3
	Summer	10	−35.6 ± 2.9		39.9 ± 65.0	
	Fall	1	−39.5 ± 0.8		29.3 ± 1.6	
Livestock	Spring	20	−37.5 ± 2.7	−34.9 ± 4.4	3,382.9 ± 1745.6	3,317.0 ± 2,316.0
	Summer	7	−28.7 ± 2.3		1775.8 ± 1,281.1	
	Fall	3	−33.9 ± 2.0		1,099.9 ± 815.4	
	Winter	4	−34.0 ± 3.8		7,364.0 ± 1,689.7	

ventilation of pig houses was increased to help cooling, which favors NH_3 dispersion. It suggests that the ventilation could be an important influence factor for NH_3 concentration in the livestock site. Moreover, human activities might also affect NH_3 emission for some source type. For example, the residential water consumption would increase in summer, and the sewage treatment plant took on heavier treatment task. The monthly processing capacity of the Yongfeng sewage treatment plant was increased from about 450,000 m^3 in June 2017 to 700,000 m^3 in July 2017, which could also contribute to enhance NH_3 emission from sewage treatment source in summer.

3.1.2 $\delta^{15}N$-NH_3 Values From Major Sources

Figure 2 presents the range of $\delta^{15}N$-NH_3 values from NH_3 emission source samples (from −43.8 to −4.2‰). All these NH_3 source samples were depleted in ^{15}N, exhibited with negative $\delta^{15}N$-NH_3 values. In general, there were no statistically significant differences among four seasons in $\delta^{15}N$-NH_3 values for all these six sources (**Supplementary Figure S2**). The NH_3 collected from traffic source has the highest $\delta^{15}N$-NH_3 values ranged from −21.3 to −4.2‰ with an average of −14.0 ± 4.9‰ (n = 12). It is significantly distinguished from other sources ($p < 0.05$) due to its relative abundance of ^{15}N. NH_3 from fertilizer, livestock, solid waste, sewage, and human feces were more depleted in ^{15}N and represented similar $\delta^{15}N$-NH_3 values (−35.0 ± 3.9‰, −34.9 ± 4.4‰, −33.6 ± 4.5‰, −34.1 ± 4.8‰, and −32.0 ± 4.6‰, respectively, see **Table 1**). These sources were most likely dominated by the process of NH_3 volatilization and appearing in similar and depleted $\delta^{15}N$-NH_3 values. It was also mentioned by Chang et al. (2016) and Stratton et al. (2019) before. Because of the kinetic isotopic fractionation associated with volatilization, lighter isotope ($^{14}NH_3$) tends to volatilize more easily than heavier isotope ($^{15}NH_3$). According to Melander and Saunders (1980), it almost always leads to the ^{15}N enrichment in substrate and ^{15}N depletion in product. So the NH_3 from volatile sources represented negative $\delta^{15}N$ values.

The comparison between this study and previous reports are shown in **Figure 3**. The results in traffic source were similar to the tunnel observation in Shanghai and downwind monitoring in Albert (−14.2 ± 2.8‰, n = 8, Chang et al., 2016; −14.9‰, n = 4, Savard et al., 2017). Comparing with the observation in Colorado (−4.6‰ and 2.2‰, n = 2, Felix et al., 2013), the average $\delta^{15}N$-NH_3 values was lower in this study. Moreover, there is no significant difference in urban waste sources between this study and the observation conducted by Chang et al. (2016). Both Beijing and Shanghai are highly developed megacities with dense population and captured with relatively advanced waste treatment facilities. It could be responsible for the similar $\delta^{15}N$-NH_3 values.

However, livestock and fertilizer show different results from other studies. Overall, the $\delta^{15}N$-NH_3 values of livestock sampled in pig houses, ranging from −41.1 to −25.7‰ (n = 34) were relatively lower than other observations (**Figure 3**). For NH_3 volatilized from fertilizer application, results in this study (−39.5 to −27.1‰, n = 17) are similar to that reported in Canada (Savard et al., 2017). The observation in cropland is much higher than that conducted by Chang et al. (2016), since the results in this study represent the NH_3 emission in cropland

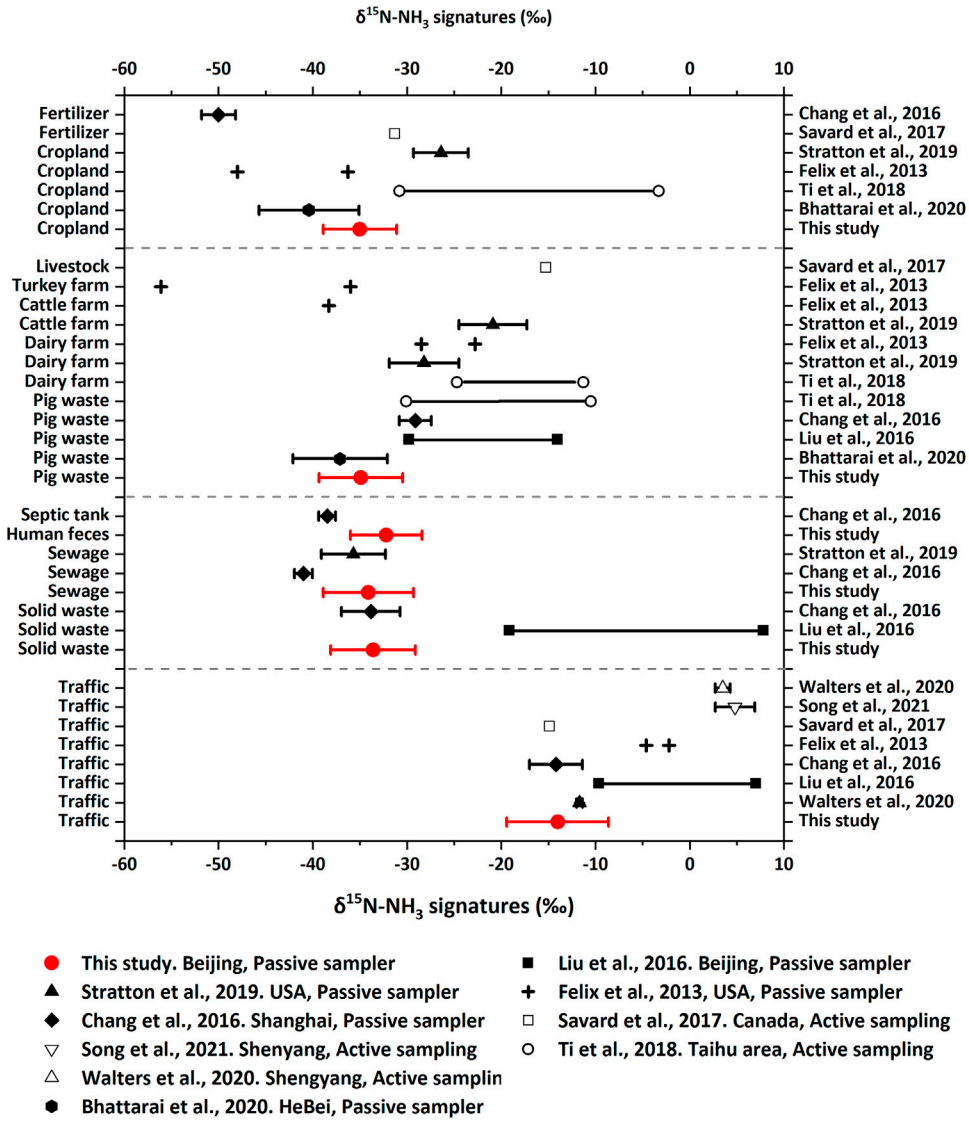

FIGURE 3 | Comparison of $\delta^{15}N$ values for major NH_3 emission sources in this study to other studies.

while Chang et al. (2016) reported laboratory results. In addition, the difference could also be due to the difference in the NH_3 sampling method. It could be found from **Figure 3** that NH_3 collected by passive samplers present lower $\delta^{15}N$ values than active sampling systems. Passive samplers trap gaseous NH_3 through diffusion, and lighter $^{14}NH_3$ is more easily diffused and adsorbed by acid coating filters. It could lead to the lower $\delta^{15}N$-NH_3 values detected by the ALPHA sampler in this study. Skinner et al. (2006) reported similar results.

3.2 Concentration and $\delta^{15}N$ Value of Ambient Ammonia

3.2.1 Concentration of Ambient Ammonia

From 26 March 2018 to 17 March 2019, the temporal variations of average concentration of ambient NH_3 are shown in **Figure 4A**. During the sampling period, the average concentration of NH_3 was 12.9 ± 6.0 μg/m^3 (ranged from 3.6 to 25.1 μg/m^3). The highest NH_3 concentration was found in 18-Jul-W2 (July 9 to 23, 2018), which was about eight times higher than the lowest determined in 18-Dec-W4 (December 24 to 31, 2018). Monthly trend of ambient NH_3 concentration is shown in **Figure 4B**. The average concentration of NH_3 increased month by month from March 2018 and reached the maximum in July 2018 (21.8 ± 4.9 μg/m^3). Then it began to decrease and fell to the lowest in winter (6.1 ± 1.9 μg/m^3, February 2019). Significant seasonal variation of NH_3 concentration could be found in **Figure 4C**. The average concentration of NH_3 in summer, spring, fall, and winter were 19.0 ± 4.5 μg/m^3, 16.1 ± 5.4 μg/m^3, 10.5 ± 2.2 μg/m^3, and 6.6 ± 1.8 μg/m^3, respectively. NH_3 concentration was relatively high in summer and spring and low in fall and winter. NH_3 emission from agricultural sources was enhanced in spring and summer, which

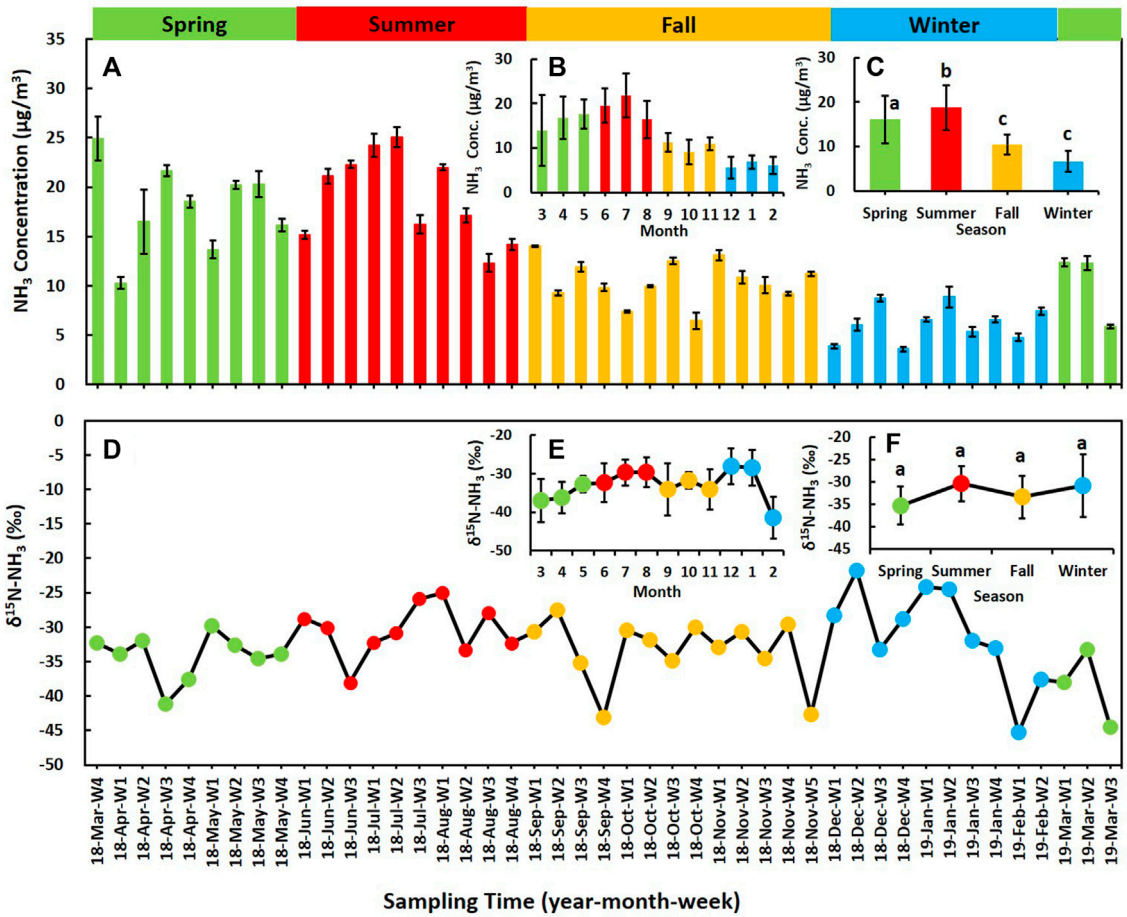

FIGURE 4 | Time series of ambient NH_3 concentration and $\delta^{15}N$ values. **(A)** shows the concentration of weekly NH_3 samples. **(B)** shows the monthly average NH_3 concentration. **(C)** shows the average concentration of NH_3 in four seasons. **(D)** shows $\delta^{15}N$ value and concentration of weekly NH_3 samples. **(E)** shows the monthly average of $\delta^{15}N$-NH_3 value. **(F)** shows the average $\delta^{15}N$-NH_3 value in four seasons. Different letters on the top of the error bars on **(C)** and **(F)** indicate significant difference in mean NH_3 concentration and insignificant difference in mean $\delta^{15}N$ values among four seasons ($p < 0.05$).

had been reported in emission inventory (Huang et al., 2012; Kang et al., 2016). It could contribute to the higher NH_3 concentration. Ambient temperature had good correlation with NH_3 concentration ($R = 0.768$, $p < 0.001$), which could be an important meteorological factor for the seasonal variation of NH_3. Higher temperature could promote the NH_3 volatilization from soil, water, and emission sources like fertilizer and livestock (Ianniello et al., 2010).

Table 2 shows the comparison of concentration of ambient NH_3 between this study and previous observation. The NH_3 concentration in urban Beijing has no significant rise in recent years. The annual average concentration of NH_3 was close to previous reports using passive samplers (13.3 μg/m^3, Zhang et al., 2018; 13.7 μg/m^3, Pan et al., 2018b). The result in winter (18.2 μg/m^3) reported by Zhao et al. (2016) was about three times higher than this study. Compared with the generally higher NH_3 concentrations in Chinese cities, there were relatively lower NH_3 concentrations in some developed regions (**Table 2**). NH_3 concentration in urban Beijing was higher than the urban sites in Spain (4.7 ± 2.1 μg/m^3, Madruga et al., 2018; 3.9 ± 2.1 μg/m^3, Reche et al., 2012) and the United States (1.8 μg/m^3, nine sites in the United States, Felix et al., 2017). It suggests that NH_3 emission intensity in Beijing could be higher than these developed countries. In the three developing sites in **Table 2**, NH_3 concentration in Beijing was close to India and lower than Egypt. It also suggests that developing areas with more serious fine particle pollution and a higher NH_3 level should pay more attention to NH_3 reduction.

3.2.2 $\delta^{15}N$ Value of Ambient Ammonia

From 26 March 2018 to 17 March 2019, the time series of the $\delta^{15}N$ value of ambient NH_3 are shown in **Figure 4D**. In general, most of the data fell within the range of $\delta^{15}N$-NH_3 values of non-traffic sources. Ranging from −44.5 to −21.8‰, the mean $\delta^{15}N$ values of ambient NH_3 was −32.7 ± 5.3‰. The mean $\delta^{15}N$-NH_3 values in summer (−30.4 ± 3.8‰) and winter (−30.9 ± 7.0‰) were slightly higher than spring (−35.3 ± 4.2‰) and fall (−33.4 ± 4.8‰). The $\delta^{15}N$-NH_3 values had no significant correlation with NH_3 concentration ($R = 0.042$, $p = 0.782$). It was also not correlated with ambient temperature in urban Beijing ($R = -0.028$, $p = 0.855$). In contrast to NH_3 concentration, no significant seasonal variation was found in $\delta^{15}N$-NH_3 values (**Figure 4F**).

TABLE 2 | Comparison of concentration and $\delta^{15}N$ values of ambient NH_3 concentration.

Location	Sampling methods	Type	Sampling period	Concentration (μg/m^3)	Reference
Beijing, China	ALPHA[a]	Urban	2018.3–2019.3	12.9	This study
		Urban	Spring, 2018	16.1	This study
		Urban	Summer, 2018	19.0	This study
		Urban	Fall, 2018	10.5	This study
		Urban	Winter, 2018	6.2	This study
		Urban	2016.3–2017.3	13.3	Zhang et al. (2018)
		Urban	Fall, 2014	9.9	Chang et al. (2016)
	Ogawa[a]	Urban	2015.9–2016.8	13.7	Pan et al. (2018b)
		Urban	Winter, 2008–2009	7.8[b]	Meng et al. (2011)
		Suburban	Winter, 2008–2009	2.5[b]	Meng et al. (2011)
	Annular diffusion denuders[c]	Urban	Winter, 2007	5.5	Ianniello et al. (2010)
		Urban	Summer, 2007	25.4	Ianniello et al. (2010)
		Urban	Summer, 2002–2003	16.6	Wu et al. (2009)
	Model 17i ammonia analyzer[d]	Urban	Winter, 2013	18.2	Zhao et al. (2016)
Xi'an, China	Ogawa[a]	Urban	Winter, 2006	6.1	Cao et al. (2009)
		Urban	Summer, 2006	20.3	Cao et al. (2009)
Shanghai, China	DOAS[d]	Urban	Winter, 2013	3.8[b]	Wang et al. (2015)
	MARGA[c]	Urban	Fall, 2012	6.6	Shi et al. (2014)
Taihu, China	Impregnated filter[e]	Urban	2014.3–2015.2	14.8	Ti et al. (2018)
		Suburban	2014.3–2015.2	19.3	Ti et al. (2018)
		Rural	2014.3–2015.2	17.2	Ti et al. (2018)
	Ogawa[a]	Urban	2015.9–2016.8	6.3	Pan et al. (2018b)
Kanpur, India	NO_x–NH_3 analyzer[d]	Urban	Winter, 2007–2008	16.3	Behera and Sharma (2010)
Kanpur, India	NO_x–NH_3 analyzer[d]	Urban	Summer, 2007–2008	18.0	Behera and Sharma (2010)
Madrid, Spain	Radiello[a]	Urban	Winter, 2014	4.7	Madruga et al. (2018)
Barcelona, Spain	ALPHA[a]	Urban	Winter, 2010	3.9	Reche et al. (2012)
United States	ALPHA[a]	Urban	2009.7–2010.6	1.8	Felix et al. (2017)
Pittsburgh, United States	ALPHA[a]	Urban	Summer, 2012	4.7	Felix et al. (2014)
Houston, United States	EC-QCL[d]	Urban	Winter, 2010	1.8[b]	Gong et al. (2011)
Cairo, Egypt	Dilute H_2SO_4 solution[c]	Suburban	Summer, 2009	44.9	Hassan et al. (2013)
		Urban	Winter, 2009	29.1	Hassan et al. (2013)

[a]*Refers to passive diffusion sampler.*
[b]*Marks the concentration converted from ppb, the conversion formula: C (μg/m^3) = C (ppb) × 17/22.4.*
[c]*Refers to active sampling using denuders.*
[d]*Refers to optical online monitoring.*
[e]*Refers to active sampling, NH_3 collected by filter impregnated of solution or absorption solution.*

In some weeks, the $\delta^{15}N$-NH_3 values was very deplete, and it even more depleted than the lowest $\delta^{15}N$-NH_3 values in the source profile (−43.8‰, in oxidation ditch, sewage treatment). N isotope fractionation could happen during the aerosol formation process, the collected NH_3 was not initial NH_3 mixing from sources. According to the previous study, aerosol formation could result in lower $\delta^{15}N$ values of collected NH_3, compared to initial gaseous NH_3. The $\delta^{15}N$-NH_3 values could decrease from −5 to −20‰ in gaseous NH_3 and increase from +5 to +20‰ in aerosol through the process of aerosol formation (Heaton et al., 1997; Pan et al., 2018a). It could also be influenced by the volatilization from unstable ammonium particles (such as NH_4NO_3 and NH_4Cl). Another reason is that possible N isotope fractionation could also occur during long-range transport of air mass (Bhattarai et al., 2021). $\delta^{15}N$-NH_3 was also dependent on the fraction (f) of the total initial gaseous NH_3 converted to NH_4^+ ion (NH_4^+/(NH_4^++NH_3)) (Heaton et al., 1997). It confirmed that $\delta^{15}N$-NH_4^+ increases with f value increases, and logically the $\delta^{15}N$ value of unconverted NH_3 would be lower. In addition, potential source contribution function analysis (PSCF) was performed to explore the possible source region and transport distance of air mass in PKU site. The principle and calculation formulas of PSCF are shown in the **Supplementary Text S1**. The whole study period was divided into two groups for PSCF analysis: $\delta^{15}N$-NH_3 values lower than −33.7‰ (the mean value of non-traffic sources) and $\delta^{15}N$-NH_3 values higher than −33.7‰. According to the results of PSCF analysis, in both of two groups, most of the air masses were arriving from the southeast areas at the PKU site. For the weeks with more depleted $\delta^{15}N$-NH_3 values, weighted PSCF values in Beijing city and its surrounding areas (**Supplementary Figure S3A**) were much lower than other weeks (**Supplementary Figure S3B**). It suggested that local emission and short-range transport of air mass may contribute less to ambient NH_3 in the PKU site, while the long-range transport of air mass from further areas may has an influence on that during these weeks. N isotope fractionation happened with the long-range transport of air mass, resulting in more depleted $\delta^{15}N$-NH_3 values.

TABLE 3 | Comparison of concentration and $\delta^{15}N$ values of ambient NH_3 concentration and $\delta^{15}N$-NH_3 values.

Location	Sampling methods	Type	Sampling period	$\delta^{15}N$-NH_3 (‰)	Reference
Beijing, China	ALPHA[a]	Urban	2018.3–2019.3	−32.7 ± 5.3[I]	This study
		Urban	Spring, 2018	−35.3 ± 4.2[I]	This study
		Urban	Summer, 2018	−30.4 ± 3.8[I]	This study
		Urban	Fall, 2018	−33.4 ± 4.8[I]	This study
		Urban	Winter, 2018	−30.9 ± 7.0[I]	This study
		Urban	2018.8–2018.9	−28.9 ± 1.5[I]	Bhattarai et al. (2020)
		Urban	2016.6–2017.3	−33.2 ± 8.6[I]	Zhang et al. (2020)
		Urban	Fall, 2014	−35.0 ± 5.4 [I]	Chang et al. (2016)
Shanghai, China	Ogawa[a]	Urban	Summer, 2015	−31.7 ± 3.4[I]	Chang et al. (2019)
	Ogawa[a]	Rural	Summer, 2015	−41.3, −36.5[I]	Chang et al. (2019)
Taihu, China	Impregnated filter[c]	Urban	2014.3–2015.2	−23.0 to −5.1[I]	Ti et al. (2018)
		Suburban	2014.3–2015.2	−24.0 to −6.0[I]	Ti et al. (2018)
		Rural	2014.3–2015.2	−24.2 to −3.0[I]	Ti et al. (2018)
Czech Republic	ALPHA[a]	Urban	Winter, 2014	−24.8[III]	Buzek et al. (2017)
		Urban	Summer, 2014	−10.3[III]	Buzek et al. (2017)
United States	ALPHA[a]	Urban	2009.7–2010.6	−15.2[II]	Felix et al. (2017)
Pittsburgh, United States	ALPHA[a]	Urban	Summer, 2012	−8.5 ± 7.2[II]	Felix et al. (2014)
Colorado, United States	Radiello[a]	Urban	2011.5–10	−16.9 ± 8.5 [II]	Stratton et al. (2019)
Colorado, United States		Rural	2011.5–10	−22.4 ± 7.3 [II]	Stratton et al. (2019)
Colorado, United States		National park	2011.5–10	−29.9 ± 3.7 [II]	Stratton et al. (2019)
Colorado, United States	Impregnated Filter[c]	Urban	/	−10.0 ± 2.6 [IV]	Moore (1977)
Niigata, Japan	Impregnated Filter[c]	Rural	2002.3–10	−14.5 to −1.0[IV]	Hayasaka et al. (2011)

I and II refer to the method based on $\delta^{15}N$-N_2O analysis, NH_4^+ was oxidized to NO_2^- by BrO^-, then converted to N_2O by I NH_2OH (Liu et al., 2014) and II bacteria (Felix et al., 2013); III and IV refer to the method based on $\delta^{15}N$-N_2 analysis, NH_3 is distilled into H_2SO_4, then converted to N_2 by III combustion (Buzek et al., 2017) and IV NaOBr (Moore, 1974).
a refers to passive sampling with diffusion sampler; c refers to active sampling, in which NH_3 was collected by filter impregnated of solution or absorption solution.

Table 3 shows the comparison of $\delta^{15}N$-NH_3 values between this study and previous reports. Compared with earlier studies using passive samplers, the determined $\delta^{15}N$-NH_3 values in this study are close to that conducted in urban Beijing (−35.0 ± 5.4‰, fall, Chang et al., 2016) and urban Shanghai (−31.7 ± 3.4‰, summer, Chang et al., 2019). However, it is lower than that reported from other foreign regions like the United States (−8.5 ± 7.2‰, Pittsburgh, Felix et al., 2014; −15.2‰, mean value in nine sites, Felix et al., 2017), Japan (−14.5 to −1.0‰, Hayasaka et al., 2011), and Czech Republic (−24.8 and −10.3‰, Buzek et al., 2017). It suggested that the source of NH_3 could be different in urban Beijing and foreign areas. Lower $\delta^{15}N$-NH_3 values in Beijing show NH_3 could more likely originate from non-traffic sources, while NH_3 in the United States could be more come from combustion-related source (like traffic). By the way, $\delta^{15}N$-NH_3 values in the urban site in Taihu areas (−23.0‰ to −5.1‰) were higher than this study in Beijing, even for the rural area (−24.2 to −3.0‰). One possible reason is the distinguished sampling methods between our studies. $\delta^{15}N$ values of NH_3 collected by active sampling systems could be higher than the passive sampler (Pan et al., 2020). It could also result from the difference of meteorological condition between Beijing and Taihu areas. The annual temperature in Taihu areas is higher than that in Beijing, which was always higher than zero in winter (Ti et al., 2018).

3.3 Source Apportionment of Ambient Ammonia

To further quantify the contribution of sources to the NH_3 in ambient air in urban Beijing using newly developed pool of $\delta^{15}N$-NH_3 signature, isotope mixing equations was applied. The $\delta^{15}N$-NH_3 source profile shows that only traffic source was significantly distinguished with other sources in $\delta^{15}N$-NH_3 value. Others sources (sewage, solid waste, human feces, fertilizer, and livestock) did not significantly differ from each other. When the $\delta^{15}N$-NH_3 values of some sources could not be significantly distinguished, they could be pooled together to reduce the number of sources (Phillips and Gregg, 2003). Therefore, these sources with close $\delta^{15}N$-NH_3 values were pooled together as the non-traffic source in calculation. The average $\delta^{15}N$-NH_3 values for traffic source and non-traffic sources (−14.0‰, and −33.7‰) were served as the baseline input to the isotope mixing equation because the $\delta^{15}N$-NH_3 values of emission source shows no significant seasonal variation in this study.

The contribution of traffic source and non-traffic source to ambient NH_3 in each week during the monitoring campaign (from 26 March 2018 to 17 March 2019) is shown in **Figure 5**. In general, the annual average contribution of traffic and non-traffic source was 8 and 92%, respectively. It suggests that NH_3 mainly comes from non-traffic source during the whole monitoring campaign in the PKU site. Considering that in some weeks the $\delta^{15}N$-NH_3 values were lower than the average of non-traffic sources and without feasible solution, the mean source proportion was figured out by putting the annual average $\delta^{15}N$ values into isotope mixing equation rather than calculating the average of weekly contribution. The weeks (19-Feb-W1 and 19-Mar-W3) in which $\delta^{15}N$-NH_3 values lower than lowest value (−43.8‰, in oxidation ditch, sewage treatment) were not included in calculation to minimize the influence of isotope fraction. The uncertainty was also assessed in this study. The standard error of source proportion was 4% for calculated source proportion of traffic and non-traffic sources. The uncertainty

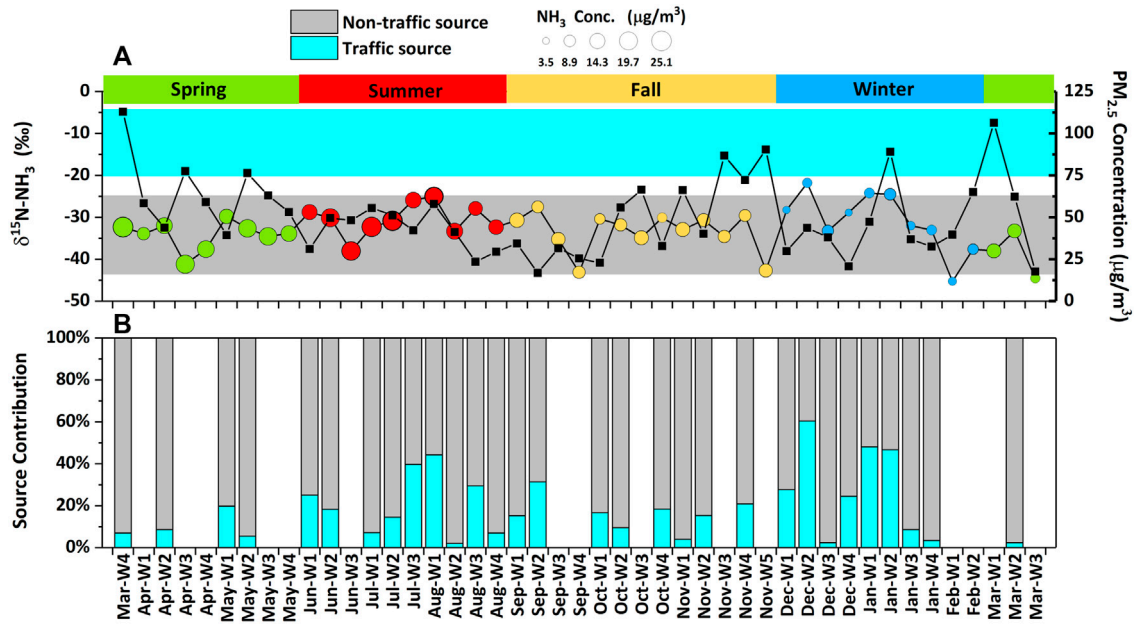

FIGURE 5 | The contribution proportion of traffic source and non-traffic sources to ambient NH_3. **(A)** shows the $\delta^{15}N$-NH_3 value, NH_3 concentration, and $PM_{2.5}$ concentration. **(B)** shows the contribution of traffic source and non-traffic sources to ambient NH_3.

assessment in source apportionment was conducted by ISOERROR (v1.04), which takes the isotope values variability of both NH_3 sources and ambient NH_3 into consideration. The principle and calculation formulas of ISOERROR are shown in the **Supplementary Text S2**, more detailed information could be found in Phillips and Gregg (2001).

The traffic source proportion to ambient NH_3 in summer, fall, and winter was 17, 2, and 22%, respectively (the stand error was 9, 8, and 14%, respectively). Although the mean $\delta^{15}N$-NH_3 in spring had no satisfactory solution and then was removed, the comparison of the mean $\delta^{15}N$-NH_3 value could also help to evaluate NH_3 sources between spring and winter qualitatively. The mean $\delta^{15}N$-NH_3 value in spring (−35.3 ± 4.2‰, ranging from −29.8 to −44.5‰) was lower than that in winter (−30.9 ± 7.0‰, ranging from −21.8 to −45.3‰), suggesting that non-traffic source may contribute more to NH_3 at sampling site. Furthermore, part of samples in spring was still available to compare the contributions of traffic emissions to NH_3 between winter and spring (**Figure 5B**), in spite that the removal of data in spring might lead to an underestimate in the contribution of non-traffic NH_3 emission sources with low $\delta^{15}N$-NH_3. It shows that traffic contributed more to ambient NH_3 in winter and summer than other seasons at the PKU site. Due to agricultural timing, NH_3 emitted from agricultural sources was reduced in winter and enhanced in spring. Low temperature was also not conducive to the volatilization of NH_3 from sources in winter. So the calculated contribution proportion of traffic was increased in winter compared with spring. Specially in winter, NH_3 reduction should be paid more attention for haze mitigation,considering that haze happened more frequently in this season.

3.4 Estimation of Source Apportionment Results

The results of sources apportionment in this study were evaluated against the online monitoring of NH_3. From March 2018 to March 2019, continuous online monitoring (hourly temporal resolution) of ambient NH_3 was conducted by the *In situ* gas and aerosol composition monitoring system (IGAC, Model S-611, Fortelice International Co., Ltd.) at the PKU site at the same time. More detailed information of IGAC could be found in Young et al. (2016). Comparison of IGAC and ALPHA in NH_3 concentration was conducted. The hourly NH_3 concentration determined by IGAC was averaged to match the time resolution of ALPHA for comparison. The NH_3 concentration monitored by IGAC was close to ALPHA passive samplers, and good correlation was found between these two methods (**Supplementary Figures S4, S5**). The results of NH_3 concentration determined by ALPHA and IGAC in this study were credible. It also suggested that NH_3 samples collected by ALPHA were effective for further isotope analysis.

Previous studies showed that the diurnal NH_3 in the different source region had a distinct daily pattern (Wang et al., 2015). The diurnal NH_3 showed a bimodal cycle in the urban area and a single peak in the rural area. It suggests that NH_3 diurnal variation could help to distinguish the major source of NH_3. By calculating the mean NH_3 concentration

observed by IGAC in each hour in a day, the NH_3 diurnal variations in four seasons during monitoring campaign are displayed in **Supplementary Figure S6**. To make sure the NH_3 diurnal drawn in this study could reveal the true trend of ambient NH_3 at the PKU site, only the days with more than 20 h effective hourly NH_3 concentration data were included in calculation. Distinct difference could be found between winter and other seasons. The single peak pattern (at 09:00–10:00) of NH_3 diurnal was found in spring, summer, and fall. Ambient temperature also shows similar diurnal trends to NH_3 concentration. It suggests NH_3 from volatile sources could play an important role in these seasons. In contrast, the NH_3 diurnal shows two peaks at 08:00–09:00 in the morning and 23:00–01:00 at the night in winter. It was consistent with traffic emission in Beijing. The NH_3 concentration peak at 23:00–01:00 could be caused by diesel trucks, because diesel trucks are only allowed to enter the fifth ring road from 23:00 at night to 6:00 the next day in Beijing. The significant difference of NH_3 diurnal between winter and other seasons suggests that the contribution of traffic to ambient NH_3 could increase in winter. It is consistent with the results by the isotope method.

Comparison between the calculated traffic contribution in this study and the results using NH_3 emission inventory was also conducted in this study. From November 2016 to March 2017, the monthly NH_3 emissions were compiled at a 1× 1 km grid by five sources (traffic, coal combustion, urban waste, fertilizer, and livestock) in the Beijing–Tianjin–Hebei region. To achieve reliable NH_3 emission calculation, native experiments results were considered and emission factors were parameterized by meteorological and other factors. More details of emission inventory could be found in previous studies (Huang et al., 2012; Kang et al., 2016). Considering that NH_3 is transported on a regional scale, the source analysis of NH_3 was based on the emission inventory in the Beijing–Tianjin–Hebei region. The emission inventory showed that the contribution of traffic, coal combustion, urban waste, fertilizer, and livestock were 15, 12, 5, 27, and 41%, respectively. From November 2018 to March 2019, the average $\delta^{15}N$ values of NH_3 were −31.6‰, the calculated contribution of traffic and non-traffic source was 11 and 89%. In general, source apportionment results of two methods in traffic were close, suggesting that the results in this study were relatively reliable.

4 CONCLUSION

Our study reported the $\delta^{15}N$ source profiles of NH_3 in urban Beijing for the first time, and the overall $\delta^{15}N$ values of NH_3 sources were −14.0 ± 4.9, −35.0 ± 3.9, −34.9 ± 4.4, −33.6 ± 4.5, −34.1 ± 4.8, and −32.0 ± 4.6‰, for traffic, fertilizer, livestock, solid waste, sewage, and human feces, respectively. No significant seasonal variation of the $\delta^{15}N$ signature of NH_3 from sources was found. The $\delta^{15}N$-NH_3 values of solid waste, sewage, human feces, fertilizer, and livestock (NH_3 volatilized from volatile nitrogen compound directly) were more depleted and overlapped, significantly different from that emitted from traffic. The mechanism of NH_3 formation could be a key influence factor of $\delta^{15}N$-NH_3 values.

In addition, the contribution of traffic and non-traffic sources to ambient NH_3 was quantified by using isotope mixing equation in urban Beijing from March 2018 to March 2019. The average contribution proportion of traffic and non-traffic sources was 8 and 92%, respectively. The contribution of traffic was increased in winter, with an average of 22%. The weekly contribution of traffic could reach to over 50%. The increased contribution of traffic to the ambient NH_3 during winter time indicating that control the NH_3 emitted from a vehicle exhaust could be meaningful to NH_3 reduction in urban Beijing.

There still exists uncertainty of source apportionment using $\delta^{15}N$. First, the $\delta^{15}N$-NH_3 values could not be significantly distinguished among fertilizer, livestock, sewage, solid waste, and human feces. Only the contribution of traffic and non-traffic sources could be figured out to a relatively reliable degree. Second, some potential sources (such as biomass burning, coal, and soil) were not involved in the source profile so far. $\delta^{15}N$ of NH_3 emitted from the volatilization of ammonium particles was hard to determine. Thus, it is still important to make the current source profile more complete. Last, the isotope fraction could happen during aerosol formation and other process. How to determine the initial $\delta^{15}N$ of mixed NH_3 from sources in ambient air is still an important task. Combining multiple methods could help to achieve more reliable source apportionment of NH_3 in the future.

DATA AVAILABILITY STATEMENT

The observed data of NH_3 source profile are available on **Supplementary Material** at https://www.frontiersin.org/articles/10.3389/fenvs.2022.903013/full#supplementary-material. Publicly available datasets were analyzed in this study. These data can be found here: http://data.cma.cn/data/detail/dataCode/A.0012.0001.html.

AUTHOR CONTRIBUTIONS

AT conceived and designed the project; MZ guided data analyses and manuscript writing; CW and XJL handled the field observation and laboratory experiments; CW and AT performed the data analyses and prepared the original draft; TZ and MC took part in the original draft writing; XM, YZ, XML, AT, MZ, and XJL reviewed and edited the manuscript; AT, MZ, and XJL were responsible for project administration and funding acquisition, and all authors joined result discussion and commented on the manuscript.

FUNDING

This work was financially supported by the National Natural Science Foundation of China (41730855, 42030708), the National Key R&D program of China (2016YFC0207906-1,

2017YFC0210101), and the High-level Innovative Talent Project of China Agricultural University.

ACKNOWLEDGMENTS

Special thanks go to Yu Song for providing the results of NH_3 emission inventory for the estimation of source apportionment results. The authors thank Zhipeng Sha and Tiantian Lv for their kind assistance in NH_3 source sampling and Yali Jin and Junyi Liu for their kind help in NH_3 online monitoring.

SUPPLEMENTARY MATERIAL

The Supplementary Material for this article can be found online at: https://www.frontiersin.org/articles/10.3389/fenvs.2022.903013/full#supplementary-material

REFERENCES

Ansari, A. S., and Pandis, S. N. (1998). Response of Inorganic PM to Precursor Concentrations. *Environ. Sci. Technol.* 32 (18), 2706–2714. doi:10.1021/es971130j

Behera, S. N., and Sharma, M. (2010). Investigating the Potential Role of Ammonia in Ion Chemistry of Fine Particulate Matter Formation for an Urban Environment. *Sci. Total Environ.* 408 (17), 3569–3575. doi:10.1016/j.scitotenv.2010.04.017

Behera, S. N., Sharma, M., Aneja, V. P., and Balasubramanian, R. (2013). Ammonia in the Atmosphere: a Review on Emission Sources, Atmospheric Chemistry and Deposition on Terrestrial Bodies. *Environ. Sci. Pollut. Res.* 20 (11), 8092–8131. doi:10.1007/s11356-013-2051-9

Bhattarai, N., Wang, S., Xu, Q., Dong, Z., Chang, X., Jiang, Y., et al. (2020). Sources of Gaseous NH_3 in Urban Beijing from Parallel Sampling of NH_3 and NH_4^+, Their Nitrogen Isotope Measurement and Modeling. *Sci. Total Environ.* 747, 141361. doi:10.1016/j.scitotenv.2020.141361

Bhattarai, N., Wang, S., Pan, Y., Xu, Q., Zhang, Y., Chang, Y., et al. (2021). δ^{15}N-stable Isotope Analysis of NHx: An Overview on Analytical Measurements, Source Sampling and its Source Apportionment. *Front. Environ. Sci. Eng.* 15 (6), 126. doi:10.1007/s11783-021-1414-6

Bouwman, A. F., Lee, D. S., Asman, W. A. H., Dentener, F. J., Van Der Hoek, K. W., and Olivier, J. G. J. (1997). A Global High-Resolution Emission Inventory for Ammonia. *Glob. Biogeochem. Cycles* 11 (4), 561–587. doi:10.1029/97GB02266

Buzek, F., Cejkova, B., Hellebrandova, L., Jackova, I., Lollek, V., Lnenickova, Z., et al. (2017). Isotope Composition of NH_3, NO_x and SO_2 Air Pollution in the Moravia-Silesian Region, Czech Republic. *Atmos. Pollut. Res.* 8 (2), 221–232. doi:10.1016/j.apr.2016.08.011

Cao, J.-J., Zhang, T., Chow, J. C., Watson, J. G., Wu, F., and Li, H. (2009). Characterization of Atmospheric Ammonia over Xi'an, China. *Aerosol Air Qual. Res.* 9 (2), 277–289. doi:10.4209/aaqr.2008.10.0043

Chang, Y., Liu, X., Deng, C., Dore, A. J., and Zhuang, G. (2016). Source Apportionment of Atmospheric Ammonia before, during, and after the 2014 APEC Summit in Beijing Using Stable Nitrogen Isotope Signatures. *Atmos. Chem. Phys.* 16 (18), 11635–11647. doi:10.5194/acp-16-11635-2016

Chang, Y., Zou, Z., Zhang, Y., Deng, C., Hu, J., Shi, Z., et al. (2019). Assessing Contributions of Agricultural and Nonagricultural Emissions to Atmospheric Ammonia in a Chinese Megacity. *Environ. Sci. Technol.* 53 (4), 1822–1833. doi:10.1021/acs.est.8b05984

Chang, Y. H. (2014). Non-Agricultural Ammonia Emissions in Urban China. *Atmos. Chem. Phys. Discuss.* 14 (6), 8495–8531. doi:10.5194/acpd-14-8495-2014

Felix, J. D., Elliott, E. M., Gish, T. J., McConnell, L. L., and Shaw, S. L. (2013). Characterizing the Isotopic Composition of Atmospheric Ammonia Emission Sources Using Passive Samplers and a Combined Oxidation-Bacterial Denitrifier Approach. *Rapid Commun. Mass Spectrom.* 27 (20), 2239–2246. doi:10.1002/rcm.6679

Felix, J. D., Elliott, E. M., Gish, T., Maghirang, R., Cambal, L., and Clougherty, J. (2014). Examining the Transport of Ammonia Emissions across Landscapes Using Nitrogen Isotope Ratios. *Atmos. Environ.* 95, 563–570. doi:10.1016/j.atmosenv.2014.06.061

Felix, J. D., Elliott, E. M., and Gay, D. A. (2017). Spatial and Temporal Patterns of Nitrogen Isotopic Composition of Ammonia at U.S. Ammonia Monitoring Network Sites. *Atmos. Environ.* 150, 434–442. doi:10.1016/j.atmosenv.2016.11.039

Gong, L., Lewicki, R., Griffin, R. J., Flynn, J. H., Lefer, B. L., and Tittel, F. K. (2011). Atmospheric Ammonia Measurements in Houston, TX Using an External-Cavity Quantum Cascade Laser-Based Sensor. *Atmos. Chem. Phys.* 11 (18), 9721–9733. doi:10.5194/acp-11-9721-2011

Gu, M., Pan, Y., Walters, W. W., Sun, Q., Song, L., and Wang, Y. (2022). Vehicular Emissions Enhanced Ammonia Concentrations in Winter Mornings: Insights From Diurnal Nitrogen Isotopic Signatures. *Environ. Sci. Technol.* 56, 1578–1585. doi:10.1021/acs.est.1c05884

Hassan, S. K., El–Abssawy, A. A., and Khoder, M. I. (2013). Characteristics of Gas-phase Nitric Acid and Ammonium-Nitrate- Sulfate Aerosol, and Their Gas-phase Precursors in a Suburban Area in Cairo, Egypt. *Atmos. Pollut. Res.* 4 (1), 117–129. doi:10.5094/APR.2013.012

Hayasaka, H., Fukuzaki, N., Kondo, S., Ishizuka, T., and Totsuka, T. (2011). Nitrogen Isotopic Ratios of Gaseous Ammonia and Ammonium Aerosols in the Atmosphere. *J. Jpn. Soc. Atmos. Environ.* 39 (6), 272–279. (in Japanese). doi:10.11298/taiki1995.39.6_272

Heaton, T. H. E., Spiro, B., Robertson, S. M. C., and Robertson, C. (1997). Potential Canopy Influences on the Isotopic Composition of Nitrogen and Sulphur in Atmospheric Deposition. *Oecologia* 109 (4), 600–607. doi:10.1007/s004420050122

Holland, E. A., Dentener, F. J., Braswell, B. H., and Sulzman, J. M. (1999). Contemporary and Pre-industrial Global Reactive Nitrogen Budgets. *Biogeochemistry* 46 (1), 7–43. doi:10.1007/BF01007572

Huang, X., Song, Y., Li, M., Li, J., Huo, Q., Cai, X., et al. (2012). A High-Resolution Ammonia Emission Inventory in China. *Glob. Biogeochem. Cycles* 26 (1). doi:10.1029/2011GB004161

Huang, R.-J., Zhang, Y., Bozzetti, C., Ho, K.-F., Cao, J.-J., Han, Y., et al. (2014). High Secondary Aerosol Contribution to Particulate Pollution during Haze Events in China. *Nature* 514 (7521), 218–222. doi:10.1038/nature13774

Huang, S., Lv, W., Bloszies, S., Shi, Q., Pan, X., and Zeng, Y. (2016). Effects of Fertilizer Management Practices on Yield-Scaled Ammonia Emissions from Croplands in China: a Meta-Analysis. *Field Crops Res.* 192, 118–125. doi:10.1016/j.fcr.2016.04.023

Ianniello, A., Spataro, F., Esposito, G., Allegrini, I., Rantica, E., Ancora, M. P., et al. (2010). Occurrence of Gas Phase Ammonia in the Area of Beijing (China). *Atmos. Chem. Phys.* 10 (19), 9487–9503. doi:10.5194/acp-10-9487-2010

Kang, Y., Liu, M., Song, Y., Huang, X., Yao, H., Cai, X., et al. (2016). High-resolution Ammonia Emissions Inventories in China from 1980 to 2012. *Atmos. Chem. Phys.* 16 (4), 2043–2058. doi:10.5194/acp-16-2043-2016

Kirkby, J., Curtius, J., Almeida, J., Dunne, E., Duplissy, J., Ehrhart, S., et al. (2011). Role of Sulphuric Acid, Ammonia and Galactic Cosmic Rays in Atmospheric Aerosol Nucleation. *Nature* 476 (7361), 429–433. doi:10.1038/nature10343

Li, M., Liu, H., Geng, G., Hong, C., Liu, F., Song, Y., et al. (2017). Anthropogenic Emission Inventories in China: a Review. *Natl. Sci. Rev.* 4 (6), 834–866. doi:10.1093/nsr/nwx150

Liu, X., Zhang, Y., Han, W., Tang, A., Shen, J., Cui, Z., et al. (2013). Enhanced Nitrogen Deposition over China. *Nature* 494 (7438), 459–462. doi:10.1038/nature11917

Liu, D., Fang, Y., Tu, Y., and Pan, Y. (2014). Chemical Method for Nitrogen Isotopic Analysis of Ammonium at Natural Abundance. *Anal. Chem.* 86 (8), 3787–3792. doi:10.1021/ac403756u

Liu, J., Zhang, Y., Liu, X., Tang, A., Qiu, H., and Zhang, F. (2016). Concentrations and Isotopic Characteristics of Atmospheric Reactive Nitrogen Around Typical Sources in Beijing, China. *J. Arid. Land* 8 (6), 910–920. doi:10.1007/s40333-016-0020-0

Liu, L., Xu, W., Lu, X., Zhong, B., Guo, Y., Lu, X., et al. (2022). Exploring Global Changes in Agricultural Ammonia Emissions and Their Contribution to Nitrogen Deposition since 1980. *Proc. Natl. Acad. Sci. U.S.A.* 119 (14), e2121998119. doi:10.1073/pnas.2121998119

Madruga, D. G., Patier, R. F., Puertas, M. A. S., García, M. D. R., and López, A. C. (2018). Characterization and Local Emission Sources for Ammonia in an Urban Environment. *Bull. Environ. Contam. Toxicol.* 100 (4), 593–599. doi:10.1007/s00128-018-2296-6

Melander, L., and Saunders, W. H. (1980). *Reaction Rates of Isotopic Molecules*. Chicheste, New York, USA: Wiley-Interscience, 12–16.

Meng, Z. Y., Lin, W. L., Jiang, X. M., Yan, P., Wang, Y., Zhang, Y. M., et al. (2011). Characteristics of Atmospheric Ammonia over Beijing, China. *Atmos. Chem. Phys.* 11 (12), 6139–6151. doi:10.5194/acp-11-6139-2011

Moore, H. (1974). Isotopic Measurement of Atmospheric Nitrogen Compounds. *Tellus* 26 (1–2), 169–174. doi:10.1111/j.2153-3490.1974.tb01963.x

Moore, H. (1977). The Isotopic Composition of Ammonia, Nitrogen Dioxide and Nitrate in the Atmosphere. *Atmos. Environ. (1967)* 11 (12), 1239–1243. doi:10.1016/0004-6981(77)90102-0

Pan, Y., Tian, S., Liu, D., Fang, Y., Zhu, X., Zhang, Q., et al. (2016). Fossil Fuel Combustion-Related Emissions Dominate Atmospheric Ammonia Sources during Severe Haze Episodes: Evidence from ^{15}N-Stable Isotope in Size-Resolved Aerosol Ammonium. *Environ. Sci. Technol.* 50 (15), 8049–8056. doi:10.1021/acs.est.6b00634

Pan, Y., Tian, S., Liu, D., Fang, Y., Zhu, X., Gao, M., et al. (2018a). Isotopic Evidence for Enhanced Fossil Fuel Sources of Aerosol Ammonium in the Urban Atmosphere. *Environ. Pollut.* 238, 942–947. doi:10.1016/j.envpol.2018.03.038

Pan, Y., Tian, S., Zhao, Y., Zhang, L., Zhu, X., Gao, J., et al. (2018b). Identifying Ammonia Hotspots in China Using a National Observation Network. *Environ. Sci. Technol.* 52 (7), 3926–3934. doi:10.1021/acs.est.7b05235

Pan, Y., Gu, M., Song, L., Tian, S., Wu, D., Walters, W. W., et al. (2020). Systematic Low Bias of Passive Samplers in Characterizing Nitrogen Isotopic Composition of Atmospheric Ammonia. *Atmos. Res.* 243, 105018. doi:10.1016/j.atmosres.2020.105018

Paulot, F., Jacob, D. J., Pinder, R. W., Bash, J. O., Travis, K., and Henze, D. K. (2014). Ammonia Emissions in the United States, European Union, and China Derived by High-resolution Inversion of Ammonium Wet Deposition Data: Interpretation with a New Agricultural Emissions Inventory (MASAGE_NH3). *J. Geophys. Res. Atmos.* 119 (7), 4343–4364. doi:10.1002/2013JD021130

Phillips, D. L., and Gregg, J. W. (2001). Uncertainty in Source Partitioning Using Stable Isotopes. *Oecologia* 127 (2), 171–179. doi:10.1007/s004420000578

Phillips, D. L., and Gregg, J. W. (2003). Source Partitioning Using Stable Isotopes: Coping with Too Many Sources. *Oecologia* 136 (2), 261–269. doi:10.1007/s00442-003-1218-3

Reche, C., Viana, M., Pandolfi, M., Alastuey, A., Moreno, T., Amato, F., et al. (2012). Urban NH_3 Levels and Sources in a Mediterranean Environmentt. *Atmos. Environ.* 57, 153–164. doi:10.1016/j.atmosenv.2012.04.021

Savard, M. M., Cole, A., Smirnoff, A., and Vet, R. (2017). δ^{15}N Values of Atmospheric N Species Simultaneously Collected Using Sector-Based Samplers Distant from Sources–Isotopic Inheritance and Fractionation. *Atmos. Environ.* 162, 11–22. doi:10.1016/j.atmosenv.2017.05.010

Sha, Z., Ma, X., Loick, N., Lv, T., Cardenas, L. M., Ma, Y., et al. (2020). Nitrogen Stabilizers Mitigate Reactive N and Greenhouse Gas Emissions from an Arable Soil in North China Plain: Field and Laboratory Investigation. *J. Clean. Prod.* 258, 121025. doi:10.1016/j.jclepro.2020.121025

Shi, Y., Chen, J., Hu, D., Wang, L., Yang, X., and Wang, X. (2014). Airborne Submicron Particulate (PM_1) Pollution in Shanghai, China: Chemical Variability, Formation/dissociation of Associated Semi-volatile Components and the Impacts on Visibility. *Sci. Total Environ.* 473-474, 199–206. doi:10.1016/j.scitotenv.2013.12.024

Skinner, R., Ineson, P., Hicks, W. K., Jones, H. E., Sleep, D., Leith, I. D., et al. (2004). Correlating the Spatial Distribution of Atmospheric Ammonia with δ^{15}N Values at an Ammonia Release Site. *Water Air Soil Pollut. Focus* 4 (6), 219–228. doi:10.1007/s11267-004-3032-2

Skinner, R., Ineson, P., Jones, H., Sleep, D., and Theobald, M. (2006). Sampling Systems for Isotope-Ratio Mass Spectrometry of Atmospheric Ammonia. *Rapid Commun. Mass Spectrom.* 20 (2), 81–88. doi:10.1002/rcm.2279

Song, L., Walters, W. W., Pan, Y., Li, Z., Gu, M., Duan, Y., et al. (2021). ^{15}N Natural Abundance of Vehicular Exhaust Ammonia, Quantified by Active Sampling Techniquess. *Atmos. Environ.* 255, 118430. doi:10.1016/j.atmosenv.2021.118430

Stratton, J. J., Ham, J., Collett, J. L., Jr, Benedict, K., and Borch, T. (2019). Assessing the Efficacy of Nitrogen Isotopes to Distinguish Colorado Front Range Ammonia Sources Affecting Rocky Mountain National Park. *Atmos. Environ.* 215, 116881. doi:10.1016/j.atmosenv.2019.116881

Sun, Y., Zhuang, G., Tang, A., Wang, Y., and An, Z. (2006). Chemical Characteristics of $PM_{2.5}$ and PM_{10} in Haze-Fog Episodes in Beijing. *Environ. Sci. Technol.* 40 (10), 3148–3155. doi:10.1021/es051533g

Sun, K., Tao, L., Miller, D. J., Pan, D., Golston, L. M., Zondlo, M. A., et al. (2017). Vehicle Emissions as an Important Urban Ammonia Source in the United States and China. *Environ. Sci. Technol.* 51 (4), 2472–2481. doi:10.1021/acs.est.6b02805

Sutton, M. A., Dragosits, U., Tang, Y. S., and Fowler, D. (2000). Ammonia Emissions from Non-agricultural Sources in the UK. *Atmos. Environ.* 34 (6), 855–869. doi:10.1016/S1352-2310(99)00362-3

Tang, Y. S., Cape, J. N., and Sutton, M. A. (2001). Development and Types of Passive Samplers for Monitoring Atmospheric NO_2 and NH_3 Concentrations. *Sci. World J.* 1, 513–529. doi:10.1100/tsw.2001.82

Ti, C., Gao, B., Luo, Y., Wang, X., Wang, S., and Yan, X. (2018). Isotopic Characterization of NH_x-N in Deposition and Major Emission Sources. *Biogeochemistry* 138 (1), 85–102. doi:10.1007/s10533-018-0432-3

Tian, S., Pan, Y., Liu, Z., Wen, T., and Wang, Y. (2014). Size-Resolved Aerosol Chemical Analysis of Extreme Haze Pollution Events during Early 2013 in Urban Beijing, China. *J. Hazard. Mater.* 279, 452–460. doi:10.1016/j.jhazmat.2014.07.023

Walters, W. W., Song, L., Chai, J., Fang, Y., Colombi, N., and Hastings, M. G. (2020). Characterizing the Spatiotemporal Nitrogen Stable Isotopic Composition of Ammonia in Vehicle Plumes. *Atmos. Chem. Phys.* 20 (19), 11551–11567. doi:10.5194/acp-20-11551-2020

Wang, S., Nan, J., Shi, C., Fu, Q., Gao, S., Wang, D., et al. (2015). Atmospheric Ammonia and its Impacts on Regional Air Quality over the Megacity of Shanghai, China. *Sci. Rep.* 5 (1), 15842. doi:10.1038/srep15842

Warner, J. X., Dickerson, R. R., Wei, Z., Strow, L. L., Wang, Y., and Liang, Q. (2017). Increased Atmospheric Ammonia over the World's Major Agricultural Areas Detected from Space. *Geophys. Res. Lett.* 44 (6), 2875–2884. doi:10.1002/2016GL072305

Wu, Z., Hu, M., Shao, K., and Slanina, J. (2009). Acidic Gases, NH_3 and Secondary Inorganic Ions in PM_{10} during Summertime in Beijing, China and Their Relation to Air Mass History. *Chemosphere* 76 (8), 1028–1035. doi:10.1016/j.chemosphere.2009.04.066

Xu, W., Luo, X. S., Pan, Y. P., Zhang, L., Tang, A. H., Shen, J. L., et al. (2015). Quantifying Atmospheric Nitrogen Deposition through a Nationwide Monitoring Network across China. *Atmos. Chem. Phys.* 15 (21), 12345–12360. doi:10.5194/acp-15-12345-2015

Xu, W., Song, W., Zhang, Y., Liu, X., Zhang, L., Zhao, Y., et al. (2017). Air Quality Improvement in a Megacity: Implications from 2015 Beijing Parade Blue Pollution Control Actions. *Atmos. Chem. Phys.* 17 (1), 31–46. doi:10.5194/acp-17-31-2017

Young, L.-H., Li, C.-H., Lin, M.-Y., Hwang, B.-F., Hsu, H.-T., Chen, Y.-C., et al. (2016). Field Performance of a Semi-continuous Monitor for Ambient PM2.5 Water-Soluble Inorganic Ions and Gases at a Suburban Site. *Atmos. Environ.* 144, 376–388. doi:10.1016/j.atmosenv.2016.08.062

Zhang, X., Wu, Y., Liu, X., Reis, S., Jin, J., Dragosits, U., et al. (2017). Ammonia Emissions May Be Substantially Underestimated in China. *Environ. Sci. Technol.* 51 (21), 12089–12096. doi:10.1021/acs.est.7b02171

Zhang, L., Chen, Y., Zhao, Y., Henze, D. K., Zhu, L., Song, Y., et al. (2018). Agricultural Ammonia Emissions in China: Reconciling Bottom-Up and Top-Down Estimates. *Atmos. Chem. Phys.* 18 (1), 339–355. doi:10.5194/acp-18-339-2018

Zhang, Y., Benedict, K. B., Tang, A., Sun, Y., Fang, Y., and Liu, X. (2020). Persistent Nonagricultural and Periodic Agricultural Emissions Dominate Sources of Ammonia in Urban Beijing: Evidence from N-15 Stable Isotope in Vertical Profiles. *Environ. Sci. Technol.* 54 (1), 102–109. doi:10.1021/acs.est.9b05741

Zhao, M., Wang, S., Tan, J., Hua, Y., Wu, D., and Hao, J. (2016). Variation of Urban Atmospheric Ammonia Pollution and its Relation with $PM_{2.5}$ Chemical Property in Winter of Beijing, China. *Aerosol Air Qual. Res.* 16 (6), 1390–1402. doi:10.4209/aaqr.2015.12.0699

Conflict of Interest: The authors declare that the research was conducted in the absence of any commercial or financial relationships that could be construed as a potential conflict of interest.

Publisher's Note: All claims expressed in this article are solely those of the authors and do not necessarily represent those of their affiliated organizations, or those of the publisher, the editors, and the reviewers. Any product that may be evaluated in this article, or claim that may be made by its manufacturer, is not guaranteed or endorsed by the publisher.